Proceedings of the 1997 IEEE
International Conference on Robotics and Automation
Albuquerque, New Mexico - April 1997

Experiments on Reaction Null-Space Based Decoupled Control of a Flexible Structure Mounted Manipulator System

D.N. Nenchev* K. Yoshida* P. Vichitkulsawat* A. Konno** M. Uchiyama*
*Department of Aeronautics and Space Engineering, Tohoku University
Aramaki-aza-Aoba, Aoba-ku, Sendai 980-77, Japan
**Department of Mechano-Informatics, University of Tokyo
Hongo 7-3-1, Bunkyo-ku, Tokyo 113, Japan

Abstract

The control of a dextrous manipulator mounted on a flexible structure is discussed. Using the concept of Reaction Null Space, the manipulator dynamics is decoupled from the base dynamics. As a consequence of the decoupling, feedback control gains for structural vibration suppression and manipulator end-point control can be determined in a straightforward manner. We examine experimentally the performance of the above control tasks, using a planar experimental setup.

1. Introduction

The interest toward complex robot systems is expanding for new application areas. An example of such a system is a dextrous manipulator mounted on a flexible base. In literature, such a system is known under the name *macro-micro system* [1]. Recently, research on macro-micro systems is gaining momentum due to two main prospective applications: nuclear waste cleanup [2], [3] and space robotics [4], [5]. We shall refer to such a system as *flexible structure mounted manipulator system (FSMS)*. We assume that the flexible base can be regarded as a passive structure. The motivation behind that is that even if the base represents another manipulator (i.e. an "active" base) such as in the case of some space robot projects, it will be used just for relocation of the dextrous manipulator. Once located at the work site, the dextrous manipulator only is controlled [6].

Two main control subtask for FSMS have been identified [7]: (1) base vibration suppression control and (2), design of control inputs that induce minimum vibrations. Another control subtask can be stated as end-point control in the presence of vibrations [8], [9]. The second control subtask has been approached from different points, e.g. through the input preshaping technique [10], the coupling map [4], [11], or through the utilization of kinematic redundancy for base motion control. A detailed treatment of the latter topic has been done by Hanson and Tolson [12]. Control inputs from the manipulator Jacobian null space have been applied, as in conventional redundancy resolution techniques. This approach yields, however, kinematic instabilities due to conflicts between the manipulator motion subtask and the base motion subtask.

In this paper we propose a control decomposition scheme based on the null space of the so-called inertia coupling matrix. We call the new framework *reaction null-space*. The reaction null-space concept has its roots in our earlier work on free-floating space robots, where the fixed-attitude-restricted (FAR) Jacobian has been proposed as a means to plan [13], [14] and control [15] manipulator motion that does not disturb the attitude of the free-floating base. Application of the reaction null space with relation to impact dynamics can be found in [16]. In a recent study [17] we emphasized the fact that the reaction null space concept is general, and can be applied to a broad class of moving base robots. The main advantage of this approach is decoupling of the interaction dynamics.

2. Background and Notation

A detailed introduction of the ideas used in this paper can be found in [18]. In this section we introduce the equation of motion of an FSMS and the concept of reaction null space.

2.1. Equation of Motion

We consider a dextrous rigid n-link manipulator attached to a flexible base in zero gravity. The *system dynamics* of the FSMS is represented in the following

0-7803-3612-7-4/97 $5.00

form:

$$\begin{bmatrix} \boldsymbol{H}_b & \boldsymbol{H}_{bm} \\ \boldsymbol{H}_{bm}^T & \boldsymbol{H}_m \end{bmatrix} \begin{bmatrix} \ddot{\boldsymbol{x}}_b \\ \ddot{\boldsymbol{\theta}} \end{bmatrix} + \begin{bmatrix} \boldsymbol{D}_b & \boldsymbol{0} \\ \boldsymbol{0} & \boldsymbol{D}_m \end{bmatrix} \begin{bmatrix} \dot{\boldsymbol{x}}_b \\ \dot{\boldsymbol{\theta}} \end{bmatrix} + \begin{bmatrix} \boldsymbol{K}_b & \boldsymbol{0} \\ \boldsymbol{0} & \boldsymbol{0} \end{bmatrix} \begin{bmatrix} \boldsymbol{x}_b \\ \boldsymbol{\theta} \end{bmatrix} + \begin{bmatrix} \boldsymbol{c}_b \\ \boldsymbol{c}_m \end{bmatrix} = \begin{bmatrix} \boldsymbol{0} \\ \boldsymbol{\tau} \end{bmatrix}, \quad (1)$$

where $\boldsymbol{x}_b \in \Re^m$ denotes the positional and orientational deflection of the base with respect to the inertial frame[1], $\boldsymbol{\theta} \in \Re^n$ stands for the manipulator generalized coordinates, $\boldsymbol{H}_b, \boldsymbol{D}_b, \boldsymbol{K}_b \in \Re^{m\times m}$ denote inertia, damping and stiffness matrices of the base, respectively, $\boldsymbol{H}_m, \boldsymbol{D}_m \in \Re^{n\times n}$ denote inertia and damping matrices of the manipulator, respectively, $\boldsymbol{c}_b$ and $\boldsymbol{c}_m$ denote velocity-dependent nonlinear terms, and $\boldsymbol{\tau} \in \Re^n$ is the joint torque. $\boldsymbol{H}_{bm} \in \Re^{m\times n}$ denotes the inertia coupling matrix. The above equation is similar to that used in [6], [11]. As it is seen, no external forces are present. Also, zero gravity environment has been assumed. We shall also assume that all submatrices of the inertia are manipulator configuration dependent only, i.e. they do not depend upon the base deflection. This simplifies the system dynamics considerably; such an approach was used by Torres and Dubowsky [4], [11] to derive the coupling map.

We shall make a final assumption to ignore the nonlinear velocity-dependent coupling terms contributed by the base deflection rate $\dot{\boldsymbol{x}}_b$. In this case, the *base dynamics* (derived from the upper part of Equation (1)) is

$$\boldsymbol{H}_b\ddot{\boldsymbol{x}}_b + \boldsymbol{D}_b\dot{\boldsymbol{x}}_b + \boldsymbol{K}_b\boldsymbol{x}_b = -\mathcal{F}, \quad (2)$$

where $\mathcal{F} = \begin{bmatrix} \boldsymbol{f}^T & \boldsymbol{t}^T \end{bmatrix}^T$ denotes the disturbance reaction force/torque induced from the manipulator motion only. This reaction is represented in the base frame as follows:

$$\mathcal{F} = \begin{bmatrix} w\ddot{\boldsymbol{r}}_{cm} \\ \frac{d}{dt}[w\boldsymbol{r}_{cm} \times \dot{\boldsymbol{r}}_{cm} + \sum_{j=1}^{n}(\boldsymbol{I}_j\boldsymbol{\omega}_j + m_j\boldsymbol{r}_j \times \dot{\boldsymbol{r}}_j)] \end{bmatrix}, \quad (3)$$

where $\boldsymbol{r}_{cm}$ denotes the manipulator center of mass position, $\boldsymbol{I}_j$, $\boldsymbol{\omega}_j$, m_j, $\boldsymbol{r}_j$ stand for the inertia matrix, angular velocity, mass and center-of-mass position for link j, respectively, and $w = \sum m_j$. The expression $\sum_{j=1}^{n}(\boldsymbol{I}_j\boldsymbol{\omega}_j + m_j\boldsymbol{r}_j \times \dot{\boldsymbol{r}}_j)$ denotes angular momentum and imposes a nonholonomic constraint. On the other hand, the upper part of Equation (3) denoting the reaction force, represents a holonomic constraint. Under the assumption pointed out earlier, namely that the inertia coupling matrix $\boldsymbol{H}_{bm}$ is regarded to be independent from the base coordinate $\boldsymbol{x}_b$, Equation (3) can be rewritten in terms of manipulator generalized coordinates, as follows:

$$\mathcal{F} = \boldsymbol{H}_{bm}\ddot{\boldsymbol{\theta}} + \dot{\boldsymbol{H}}_{bm}\dot{\boldsymbol{\theta}}. \quad (4)$$

This shows some similarity to a free-floating system. Note also that Equation (4) can be integrated:

$$\mathcal{L} = \boldsymbol{H}_{bm}\dot{\boldsymbol{\theta}}. \quad (5)$$

This integral has been called *the coupling momentum of FSMS* [18].

2.2. Reaction Null-Space and Reactionless Motion of FSMS

From Equations (4) and (5) it is apparent that the manipulator will not induce any reaction to the base if and only if the coupling momentum is conserved ($\mathcal{L}$ =const$\Leftrightarrow$ $\mathcal{F} = \boldsymbol{0}$). Let us assume that $n > m$ holds, which denotes a kinematic redundancy condition with respect to the base motion task [14]. Then, at a manipulator configuration $\tilde{\boldsymbol{\theta}}$ such that rank $\boldsymbol{H}_{bm}(\tilde{\boldsymbol{\theta}}) = \max_{\theta}$ rank $\boldsymbol{H}_{bm}(\boldsymbol{\theta})$:

1. Zero reaction is achieved with the joint acceleration

$$\ddot{\boldsymbol{\theta}}_c = -\boldsymbol{H}_{bm}^{+}\dot{\boldsymbol{H}}_{bm}\dot{\boldsymbol{\theta}} + (\boldsymbol{E} - \boldsymbol{H}_{bm}^{+}\boldsymbol{H}_{bm})\boldsymbol{\zeta} \quad (6)$$

   where $\boldsymbol{H}_{bm}^{+} \in \Re^{n\times m}$ denotes the Moore-Penrose generalized inverse of the inertia coupling matrix, $\boldsymbol{E} \in \Re^{n\times n}$ stands for the unit matrix, $\dot{\boldsymbol{\theta}}$ and $\boldsymbol{\zeta} \in \Re^n$ are arbitrary.

2. Coupling momentum conservation is achieved with the joint velocity

$$\dot{\boldsymbol{\theta}}_c = \boldsymbol{H}_{bm}^{+}\bar{\mathcal{L}} + (\boldsymbol{E} - \boldsymbol{H}_{bm}^{+}\boldsymbol{H}_{bm})\boldsymbol{\zeta} \quad (7)$$

   where $\boldsymbol{\zeta}$ denotes again an arbitrary vector, and $\bar{\mathcal{L}}$ =const.

This follows from the fact that $\ddot{\boldsymbol{\theta}}_c$ and $\dot{\boldsymbol{\theta}}_c$ are general solutions of Equations (4) and (5), respectively. The condition for maximum rank of the inertia coupling matrix is in fact a controllability condition, as discussed by Spong with regard to passive-joint manipulators [19]. Below we refer to the maximum rank case as *well-conditioned inertial coupling*; otherwise the configuration of the FSMS will be characterized as *ill-conditioned inertial coupling*.

The expression $\boldsymbol{P}_{RNS} \equiv (\boldsymbol{E} - \boldsymbol{H}_{bm}^{+}\boldsymbol{H}_{bm})$ appearing in both Equations (6) and (7), stands for the projector onto the null space of the inertia coupling matrix. This null space is called *the reaction null-space of FSMS*. The reaction null space is not zero, because we introduced the kinematic redundancy condition $n > m$

[1] Generally, $m = 6$ ($n \geq m$).

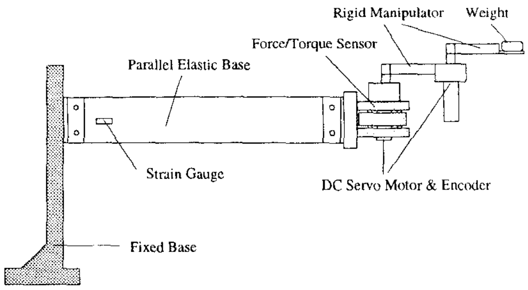

Figure 1. The experimental FSMS TREP.

above. We note, however, that also other assumptions can be made, which would assure the existence of this null space [18].

It is apparent that, with zero initial coupling momentum, zero reaction is obtained with the velocity $\dot{\boldsymbol{\theta}}_{RNS} = \boldsymbol{P}_{RNS}\boldsymbol{\zeta}$. We are interested in the component $\dot{\boldsymbol{\theta}}_{RNS}$ especially from the standpoint of integrability. At each manipulator configuration $\boldsymbol{\theta}$, the columns of the null space projector $\boldsymbol{P}_{RNS}(\boldsymbol{\theta})$ induce a smooth co-distribution [20] in joint space. If at the given configuration the inertial coupling is well-conditioned, then the co-distribution is nonsingular. According to Frobenius' theorem, a distribution is completely integrable, if and only if it is involutive. Involutivity can be examined via Lie brackets on the columns of $\boldsymbol{P}_{RNS}$. If such involutivity can be established, then the reaction null space component of the joint velocity will be integrable. The integral of $\dot{\boldsymbol{\theta}}_{RNS}$, if it exists, is called *the set of reactionless paths of an FSMS.* The reactionless paths guarantee decoupling between the base dynamics and the manipulator dynamics. We note that these paths differ from the minimum-disturbance paths of the coupling map [4]. The main advantage of the reactionless paths is that they can be generated on-line, without using a graphical tool. Unfortunately, integrability cannot be always guaranteed. The only case when integrability is guaranteed, is that of a one-dimensional distribution (*i.e.*, $n - m = 1$). Nevertheless, in some important practical cases the system can be recast to fit into this category.

3. TREP: An Experimental FSMS

In this section we shall introduce the experimental setup of our FSMS called TREP, and derive its analytical model. The experimental setup consists of a small 2R rigid link manipulator attached to the free end of a flexible double beam representing an elastic base (Figures 1 and 2). The manipulator is driven by DC servomotors with velocity command input.

The TREP FSMS is modeled according to Figure

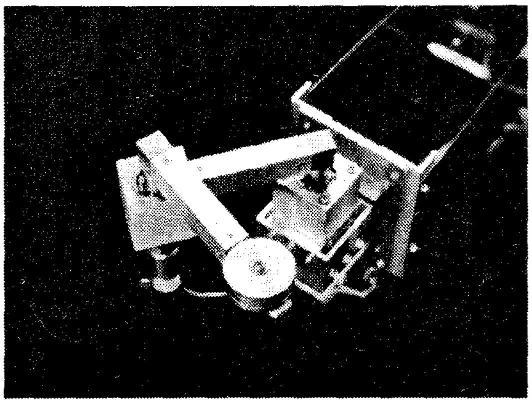

Figure 2. Photo of the experimental FSMS TREP.

3. The parameters of the manipulator and the base are presented in Tables 1 and 2, respectively. Since the elastic base has been designed as a double beam, the reaction torque can be neglected as a disturbance. This is also the case with the reaction force component along the longitudinal axis of the base. Thus, we shall consider just the reaction force along the so-called low stiffness direction, which coincides with the x axis of the elastic-base coordinate frame. This means that $m = 1$. Since the manipulator has two motors ($n = 2$), the reaction null space is one-dimensional, meaning that there is one nonzero vector in the reaction null space. Recalling the derivation in the previous section, it should be apparent that the inertia coupling matrix of this model can be determined from the equation for the velocity $\dot{r}^x_{cm}$ of the manipulator center of mass, projected onto the low-stiffness axis. This is written as

$$w\dot{r}^x_{cm} = \boldsymbol{h}_{bm} \begin{bmatrix} \dot{\theta}_1 \\ \dot{\theta}_2 \end{bmatrix} = \mathcal{L}, \tag{8}$$

where $\boldsymbol{h}_{bm} = \begin{bmatrix} h_{bm1} & h_{bm2} \end{bmatrix}$ denotes the coupling matrix, with

$$h_{bm1} = -(m_1 l_{g1} + m_2 l_1) sin(\theta_1) - m_2 l_{g2} \sin(\theta_1 + \theta_2),$$
$$h_{bm2} = -m_2 l_{g2} \sin(\theta_1 + \theta_2).$$

The reaction null space vector becomes then

$$\boldsymbol{n} = \begin{bmatrix} h_{bm2} & -h_{bm1} \end{bmatrix}^T. \tag{9}$$

A zero initial coupling momentum will be conserved with any joint velocity parallel to the reaction null space vector. This vector induces a one-dimensional co-distribution in joint space, which, with well-conditioned coupling, is integrable. Consequently, the set of reactionless paths of the system can be obtained. This set is displayed in Figure 4.

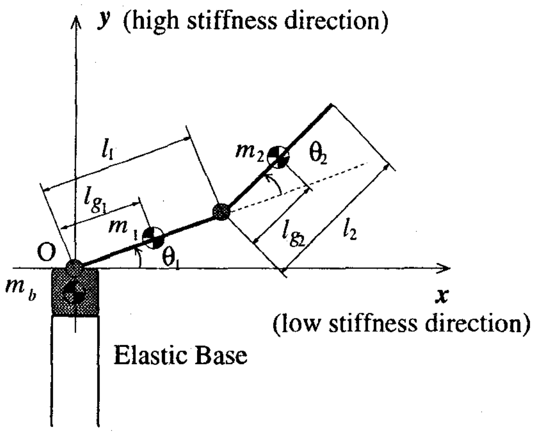

Figure 3. The model of TREP.

Table 1. Manipulator link parameters

l_1	0.1	[m]
l_2	0.1	[m]
lg_1	0.096	[m]
lg_2	0.090	[m]
m_1	0.310	[kg]
m_2	0.120	[kg]

4. Control Law Derivation

The derivation of the control law follows in general the derivation presented in [18]. However, we have to take into account that the motor drivers of TREP admit a velocity command input. That is, we shall *not* make use of the lower part of the equation of motion (1) which involves the joint torques.

As shown in [18], because of the dynamics decoupling ability of the reaction null space, it is possible to design the base vibration suppression control loop and the end-point control loop independently.

4.1. Base Vibration Suppression Control

From the base dynamics Equation (2) and the reaction dynamics Equation (4), we have

$$m_b\ddot{x}_b + k_b x_b + \dot{\boldsymbol{h}}_{bm}\dot{\boldsymbol{\theta}} = -\boldsymbol{h}_{bm}\ddot{\boldsymbol{\theta}} \tag{10}$$

Table 2. Elastic base parameters

length	0.5	[m]
hight	0.08	[m]
thickness	0.0007	[m]
beam interval	0.1	[m]
tip mass m_b	0.795	[kg]
stiffness k_b	77.9218	[N/m]

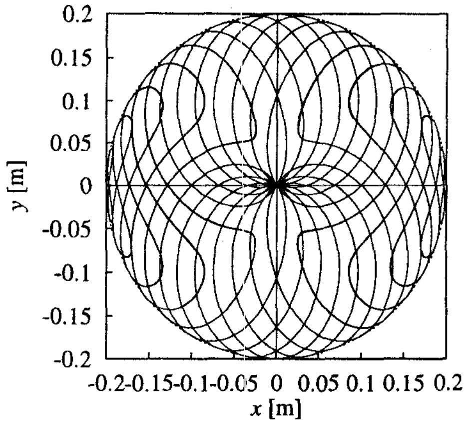

Figure 4. Reactionless paths of TREP.

where x_b denotes the deflection of the base from its equilibrium point. The natural damping of the base has been neglected. Also, the nonlinear term c_b has been represented just by the component $\dot{\boldsymbol{h}}_{bm}\dot{\boldsymbol{\theta}}$. The form of this equation is the same as that for vibration suppression control of a flexible link manipulator [21]. Therefore, we can propose a similar control law: use the command input $\dot{\boldsymbol{v}}_c = \ddot{\boldsymbol{\theta}}$:

$$\dot{\boldsymbol{v}}_c = \boldsymbol{h}_{bm}^{+}(g_f\dot{x}_b - \dot{\boldsymbol{h}}_{bm}\dot{\boldsymbol{\theta}}) \tag{11}$$

where g_f is the control gain for base vibration suppression. Under the assumption of well-conditioned inertial coupling, which is expressed as $\boldsymbol{h}_{bm} \neq \boldsymbol{0}^T$, the closed-loop system becomes

$$\ddot{x}_b + \frac{g_f}{m_b}\dot{x}_b + \frac{k_b}{m_b}x_b = 0. \tag{12}$$

With a proper (positive) g_f we obtain a damped vibration system, and hence, vibration suppression will be guaranteed.

Finally, we note that the pseudoinverse $\boldsymbol{h}_{bm}^{+}$ ensures the most efficient (in a least-squares sense) inertial coupling between the base and the manipulator [18].

4.2. Composite Control

The base vibration suppression control law is generally of the same form as that proposed by Book and Lee for FSMS [6], and by Uchiyama and Konno for a flexible link manipulator[2] [21]. As noted by those authors, the control law (11) can be superimposed to a manipulator joint-space nonlinear control law, provided the gains are selected with special care [6]. Considering a reaction null space component of the form $b\boldsymbol{n}$, b denoting

[2] In their case, the left pseudoinverse had to be used, however.

an arbitrary variable, the composite control law is:

$$\dot{\boldsymbol{v}}_c=\boldsymbol{h}_{bm}^{+}(g_f\dot{x}_b-\dot{\boldsymbol{h}}_{bm}\dot{\boldsymbol{\theta}})+b\boldsymbol{n}-\boldsymbol{G}_d\dot{\boldsymbol{\theta}}. \tag{13}$$

Because of the orthogonality between the two terms $\boldsymbol{h}_{bm}^{+}(\bullet)$ and $b\boldsymbol{n}$, it is clear that they will not influence each other. Therefore, with the above composite control law, there is no need to consider special feedback-gain design strategies. As far as the term $-\boldsymbol{G}_d\dot{\boldsymbol{\theta}}$ on the r.h.s. of Equation (13) is concerned, it should be noted that, in an idealized FSMS without energy dissipation, base vibration suppression loads the manipulator with nonzero coupling momentum. After suppressing the vibration, this momentum would be conserved, and hence, the manipulator would "float" continuously. This is avoided by means of the joint damping component $-\boldsymbol{G}_d\dot{\boldsymbol{\theta}}$. The idea is similar to the idea behind the well-known *direct velocity feedback control* of flexible structures' vibrations [22]. Magee and Book [23], [24] used a direct velocity feedback control loop for an FSMS, which was motivated by the need of extra damping and to obtain a transfer function with no finite zeros. Sharf [25] used a switched joint damping term, after vibration suppression has been completed. We must also note here that the problem of the "floating" manipulator cannot be solved by introducing additional kinematic degrees of freedom; the end-effector could thereby come to rest, the internal links, however, would continue to "float."

The fact that the reaction null space is one-dimensional, shows that there is only one degree-of-freedom left for the end-point control. This degree-of-freedom is realized as any desired (scalar) acceleration along the reactionless path. In practice this means that even very high velocity/acceleration would be admissible, as long as the motion does not deviate from the current reactionless path.

In our case, however, the composite control (13) cannot be applied directly because the motor drivers of TREP admit velocity commands. This problem is solved by integrating the control. Thereby we assumed $\boldsymbol{h}_{bm}$ to be constant, which is justified if one considers the fact that x_b can be regarded as a "fast" variable. This means that the nonlinear term $\dot{\boldsymbol{h}}_{bm}\dot{\boldsymbol{\theta}}$, and hence, the nonlinear coupling in general (i.e. the whole term $\boldsymbol{c}_b$) is ignored. The approximate integral form of the composite control (13) becomes

$$\boldsymbol{v}_c=g_f\boldsymbol{h}_{bm}^{+}x_b+g_d\left(\int\bar{b}\boldsymbol{n}dt-\boldsymbol{\theta}\right), \tag{14}$$

where $\boldsymbol{G}_d=g_d\boldsymbol{E}$, $\bar{b}=bg_d^{-1}$. It is apparent that the reference reactionless path (determined by the integral in Equation (14)) is tracked under position feedback control, making use of the gain g_d. Note that such representation was possible, since $\bar{b}$ can be chosen arbitrarily.

5. Experiments

We have conducted a series of experiments for vibration suppression, reactionless path tracking and composite control. In all the experiments, the initial configuration was the same: the arm was extended and aligned with the flexible base ($\theta_1=\theta_2=0$).

5.1. Vibration Suppression

This experiment was performed at a fixed configuration, coinciding with the initial configuration mentioned above. The control law (14) was used, where the integral was replaced by the joint angles values of the fixed configuration. The position control gain was selected to be relatively small: we used g_d=20 s^{-1}. The vibration gain was chosen as g_f=24 s^{-1}. An arbitrary external force input was applied. Figures 5a and 5b show the results for the cases with and without vibration suppression, respectively. The effectiveness of the vibration suppression was confirmed.

5.2. Reactionless Motion

The same vibration suppression feedback gain was used (g_f=24 s^{-1}). The position feedback gain was increased to g_d=50 s^{-1}. The reactionless end-point reference path is shown in the upper part of Figure 6. This path is generated on-line, by the integral term $\int\bar{b}\boldsymbol{n}dt$ (cf. Equation (14)). The (scalar) velocity on the path was determined from the variable $\bar{b}$, which was designed as a fifth-order spline function of time. In order to verify the possibility for an arbitrary choice of $\bar{b}$, we performed the motion on the same path twice, with different velocities (called fast and slow). The lower three graphs in Figure 6 show the results. It is seen that almost no base vibration is excited in both cases, and in spite of the significant difference in the joint velocity. For comparison, Figure 7 shows a point-to-point motion path (in fact, just joint two rotation) with the same boundary conditions as in the previous motion. The base vibrates significantly.

5.3. Reactionless Motion and Vibration Suppression

The same reference reactionless path as in the previous experiment was used, which was tracked however in a cyclic manner. After accelerating the arm smoothly, the variable $\bar{b}$ was kept constant as $\bar{b}=30$. During the tracking, an external force was applied to the system. Figure 8a and Figure 8b display the results in the case with and without vibration suppression control, respectively. In the first case, we see that base

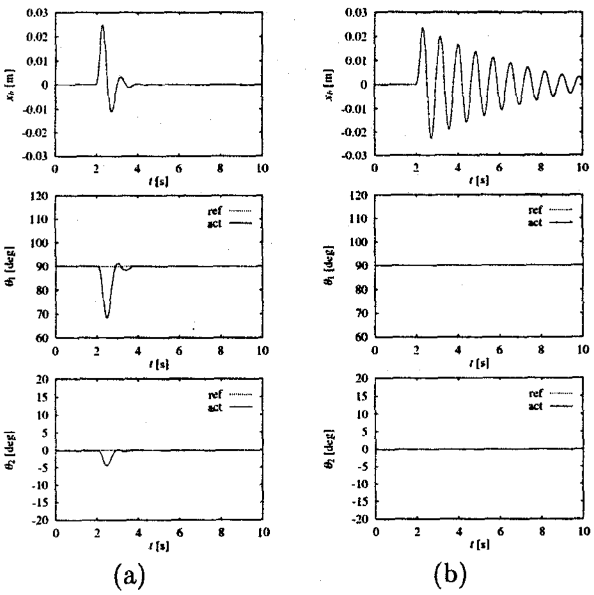

Figure 5. Base vibration: (a) with vibration suppression; (b) without vibration suppression.

vibration is very effectively suppressed, and the joint motion continues to track the reactionless path. In the case without vibration suppression, it is interesting to note that the vibration of the base is not "disturbed" at all through the joint motion. This clearly demonstrates the dynamic decoupling ability of the control.

6. Conclusions

In this paper we applied the concept of reaction null space based control of FSMS [16]–[18] to our experimental FSMS. We proposed a simplified control law and examined its performance in a vibration suppression task, a reactionless end-point control task and combined motion control task. In all cases the performance of the system was satisfactory. The design of the control gains is not critical since the two tasks are totally decoupled. We observed also a robust behavior with respect to model parameter variation, which can be explained with the same reasoning. In another work [26] we proposed and examined a reactionless path planning technique for the FSMS, and compared it to the coupling map [4] path planning technique. In a future work we plan to introduce more degrees-of-freedom attached to the flexible structure and to develop a real-time control system for reactionless teleoperation.

Acknowledgments

The authors are grateful to Koyu Abe, Toshio Miwa and Shigeru Okada for their help in designing TREP.

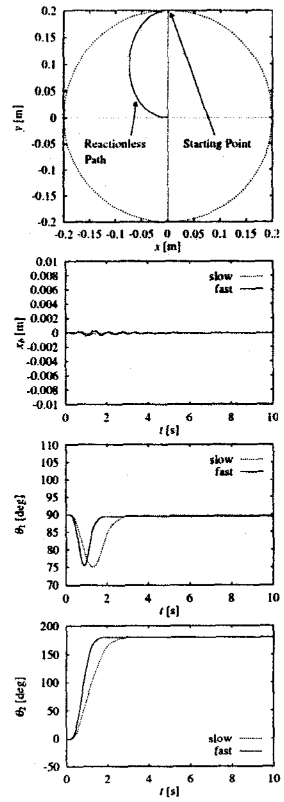

Figure 6. Reactionless path motion.

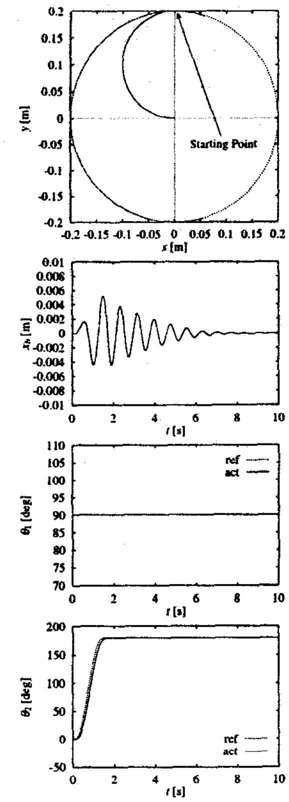

Figure 7. Point-to-point path motion.

The support through the Ippan C Research Project 07805027 Grand-in-Aid for Scientific Research from the Ministry of Education, Science and Culture of Japan is also acknowledged.

References

[1] A. Sharon and D. Hardt, "Enhancement of robot accuracy using end-point feedback and a macro-micro manipulator system," in Proc. ACC, San Diego, CA, 1984, pp. 1836–1842.

[2] J. F. Jansen et al., "Long-reach manipulation for waste storage tank remediation," DSC–Vol. 31, ASME, pp. 67–73, 1991.

[3] D.-S. Kwon et al., "Input shaping filter methods for the control of structurally flexible, long-reach manipulators," in Proc. IEEE Int. Conf. Robotics and Automation, San Diego, CA, 1994, pp. 3259–3264.

[4] M. A. Torres and S. Dubowsky, "Path-planning in elastically constrained space manipulator systems," in Proc. IEEE Int. Conf. Robotics and Automation, Atlanta, Georgia, 1993, pp. 812–817.

[5] C. Vallancourt and C. M. Gosselin, "Compensating for the structural flexibility of the SSRMS with the SPDM," 2nd Workshop on Robotics in Space, Canadian Space Agency, Montreal, Canada, July 1994.

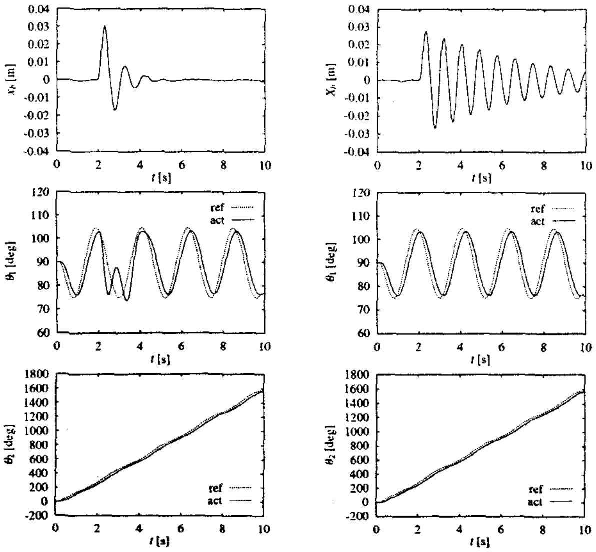

(a) (b)

Figure 8. Cyclic reactionless motion and base vibration: (a) with vibration suppression; (b) without vibration suppression.

[6] W. J. Book and S. H. Lee, "Vibration control of a large flexible manipulator by a small robotic arm," in Proc. ACC, Pittsburgh, PA, 1989, pp. 1377–1380.

[7] D. W. Cannon, D. P. Magee and W. J. Book, "Experimental study on micro/macro manipulator vibration control," in Proc. IEEE Int. Conf. Robotics and Automation, Minneapolis, MN, 1996, pp. 2549–2554.

[8] R. H. Cannon, Jr. and E. Schmitz," Initial experiments on the end-point control of a flexible one-link robot," Int. J. Rob. Res., Vol. 3, No.3, pp. 62–75, Fall 1984.

[9] C. Mavroidis, S. Dubowsky and V. Raju, "End-point control of long reach manipulator systems," in Proc. Ninth World Congress of IFToMM, Milano, Italy, 1995, pp. 1740–1744.

[10] P. H. Meckl and W. P. Seering, "Reducing residual vibration in systems with time-varying resonances," in Proc. IEEE Int. Conf. Robotics and Automation, Raleigh, NC, 1987, pp. 1690–1695.

[11] M. A. Torres, "Modelling, path-planning and control of space manipulators: the coupling map concept," Ph.D. Thesis, MIT, 1993.

[12] M. L. Hanson and R. H. Tolson, "Reducing flexible base vibrations through local redundancy resolution," J. Rob. Syst. Vol. 12, No. 11, pp. 767–779, 1995.

[13] D. N. Nenchev, K. Yoshida, and Y. Umetani, "Analysis, design and control of free-flying space robots using fixed-attitude-restricted Jacobian matrix," Robotics Research: The Fifth International Symposium, Ed. by H. Miura and S. Arimoto, The MIT Press, 1990, pp. 251–258.

[14] D. N. Nenchev, Y. Umetani, and K. Yoshida, "Analysis of a redundant free-flying spacecraft/manipulator system," IEEE Trans. Rob. Automation, Vol. 8, No. 1, pp. 1–6, Febr. 1992.

[15] D. N. Nenchev, "A controller for a redundant free flying space robot with spacecraft attitude/manipulator motion coordination," in Proc. IEEE/RSJ Int. Conf. Intelligent Robots and Systems (IROS '93), Yokohama, Japan, 1993, pp. 2108–2114.

[16] K. Yoshida and D. N. Nenchev, "Space robot impact analysis and satellite-base impulse minimization using reaction null space," in Proc. IEEE Int. Conf. Robotics and Automation, Nagoya, Japan, 1995, pp. 1271–1277.

[17] K. Yoshida, D. N. Nenchev and M. Uchiyama, "Moving base robotics and reaction management control," Robotics Research: The Seventh International Symposium, Ed. by G. Giralt and G. Hirzinger, Springer Verlag, 1996, pp. 101–109.

[18] D. N. Nenchev, K. Yoshida and M. Uchiyama, "Reaction null-space based control of flexible structure mounted manipulating systems," in Proc. 35th IEEE CDC, Kobe, Japan, 1996, pp. 4118–4123.

[19] M. W. Spong, "Partial feedback linearization of underactuated mechanical systems," in Proc. IEEE/RSJ Int. Conf. Intelligent Robots and Systems (IROS '94), 1994, Munich, Germany, pp. 314–321.

[20] A. Isidori. Nonlinear Control Systems. Third Edition. Springer Verlag, 1995.

[21] M. Uchiyama and A. Konno, "Modeling, controllability and vibration suppression of 3D flexible robots," Robotics Research: The Seventh International Symposium, Ed. by G. Giralt and G. Hirzinger, Springer Verlag, 1996, pp. 90–99.

[22] M. J. Balas, "Direct velocity feedback control of large space structures," J. Guid. Control, Vol. 2, No. 3, pp. 252–253, 1979.

[23] D. P. Magee and W. J. Book, "Filtering Schilling manipulator commands to prevent flexible structure vibration," in Proc. ACC, Baltimore, ML, 1994, pp. 2538–2542.

[24] D. P. Magee and W. J. Book, "Filtering micro-manipulator wrist commands to prevent flexible base motion," in Proc. ACC, Seattle, Washington, 1995, pp. 924–928.

[25] I. Sharf, "Active damping of a large flexible manipulator with a short-reach robot," in Proc. ACC, Seattle, Washington, 1995, pp. 3329–3333.

[26] K. Yoshida, D. N. Nenchev, P. Vichitkulsawat, H. Kobayashi, and M. Uchiyama, "Experiments on the PTP operations of a flexible structure mounted manipulator system," in Proc. IEEE/RSJ Int. Conf. on Intelligent Robots and Systems (IROS '96), Osaka, Japan, 1996, pp. 246–251.